Modeling of damage generation mechanisms in silicon at energies below the displacement threshold

Iván Santos,* Luis A. Marqués, and Lourdes Pelaz
Departamento de Electricidad y Electrónica, Universidad de Valladolid, E.T.S.I. de Telecomunicación, 47011 Valladolid, Spain
(Received 28 July 2006; revised manuscript received 12 September 2006; published 21 November 2006)

We have used molecular dynamics simulation techniques to study the generation of damage in Si within the low-energy deposition regime. We have demonstrated that energy transfers below the displacement threshold can produce a significant amount of damage, usually neglected in traditional radiation damage calculations. The formation of amorphous pockets agrees with the thermal spike concept of local melting. However, we have found that the order-disorder transition is not instantaneous, but it requires some time to reach the appropriate kinetic-potential energy redistribution for melting. The competition between the rate of this energy redistribution and the energy diffusion to the surrounding atoms determines the amount of damage generated by a given deposited energy. Our findings explain the diverse damage morphology produced by ions of different masses.

DOI: 10.1103/PhysRevB.74.174115 PACS number(s): 64.60.Cn, 61.72.Bb, 61.82.Fk

I. INTRODUCTION

There is a renewed interest in the modeling of amorphization in Si due to the use of high dopant doses and preamorphizing implants for the fabrication of integrated circuits. As dimensions are scaled down, effects such as the electrical deactivation and transient enhanced diffusion of dopants become important as they degrade the electrical characteristics of the manufactured devices. These effects are produced by the diffusion and complex interactions between dopant and lattice defects.[1,2] Consequently, it has become of fundamental importance to correctly describe not only the dopant profile, but also the profile and typology of generated damage, both in amorphizing and subamorphizing conditions.

When an ion penetrates into a solid target, it loses its energy through collisions with its atoms and electrons. Si amorphization is the result of the accumulation of damage generated within these collisions. Generally, energy transfers to the electronic system are taken as inelastic loses and do not contribute to damage generation. Only energy deposited in the form of nuclear collisions is taken into account.[3,4] Simple models describe this damage in terms of pairs of Si self-interstitials and vacancies, called Frenkel pairs. The modified Kinchin-Pease (KP) model[5] evaluates the average number of Frenkel pairs generated by the ion as $N_D = 0.42 F_D / E_d$, where F_D is the total energy deposited into nuclear collisions and E_d is the threshold energy necessary to produce a displaced atom within the target. For Si, experimental and theoretical estimations for this energy range from 11 to 30 eV,[6,7] but for most simulators it is conventionally taken as 15 eV.[8,9] According to this expression, the average number of generated Frenkel pairs does not depend on energy densities for the same nuclear deposited energy. On the other hand, the binary collision approximation (BCA) model provides an atomistic description of the implantation process but only interactions between pairs of atoms are considered. In this model, a target atom is displaced from its lattice position when it receives in a collision an energy higher than the displacement energy threshold E_d.[10] Then this target atom can create a subcascade leaving behind a vacancy and generating an interstitial defect where it stops. For energy transfers below E_d no Frenkel pairs are generated, and energy is assumed to be lost to phonons.[8]

Models based on KP and BCA adequately reproduce the dilute damage generated by light ions[4] and give reasonably good depth profiles of implanted species with very low computational cost.[9] However, they are not able to describe more complex damage structures, known as amorphous pockets, which have been experimentally observed after heavy ion implantation.[11] To correctly reproduce the formation of these amorphous pockets it is necessary to resort to more sophisticated simulation techniques such as molecular dynamics (MD),[4,12–14] where many-body interactions at any energy level (above or below E_d) are naturally included. However, this technique is computationally very expensive and consequently it is limited to relatively small systems and very short simulation times. Some efforts have been made in the past to accelerate the MD calculations in order to be able to simulate the implantation process even at implant energies as high as 100 keV.[15,16] Introduced approximations are meant to obtain dopant profiles in very good agreement with experiments, but at the expense of lacking a correct description of lattice damage.

The microelectronics industry demands ion-implant atomistic simulators with the computational efficiency of BCA but including a damage description as good as it is provided by full MD, besides having predictive capabilities.[17] To achieve such a simulator it is important to previously study and determine the underlying physical mechanisms that lead to amorphization in Si. Although damage formation processes at energies higher than E_d are fairly well known (ballistic regime[18]), that is not the case for the low-energy regime.[19,20] Our work will focus on a systematic study of damage generation at energies below E_d by the use of MD techniques. Our goals are the quantification of this damage formation mechanism and the determination of the conditions that lead to the generation of amorphous pockets.

II. BCA AND MD SIMULATIONS

In a previous work we carried out MD and BCA simulations of B, Si, and Ge (light, medium, and heavy ion types,

 ©2006 The American Physical Society

TABLE I. Mean size and energy of groups of atoms that have received energy transfers below E_d in BCA simulations of B, Si, and Ge cascades into Si with a nuclear deposited energy of 1 keV.

	Size	Energy (eV)
B	15	92
Si	29	180
Ge	50	311

respectively) cascades into Si with 1 keV of nuclear deposited energy in order to study the similarities and differences in the obtained damage structures.[21] In BCA, the number of produced Frenkel pairs was the same for the three ions, because damage production within this model depends only on the nuclear deposited energy and not on ion mass. However, the amount of damage and its complexity increased with ion mass in MD simulations. In order to investigate on the origin of this different behavior we have carried out a more detailed analysis of the energy transfers to atoms during a cascade in BCA simulations. We found that only around 23% of the nuclear deposited energy is employed to produce Frenkel pairs, independently of ion mass. The remaining percentage, 77%, is employed in energy transfers to target atoms below the displacement threshold E_d. We grouped these target atoms within a second-neighbor distance and we found that both the mean group size and the mean group energy increase with ion mass (see Table I). This dependence with ion mass is similar to the one obtained using MD techniques,[21] which suggests that low energy transfers to neighboring target atoms could have some influence on the generation of damage. In this paper we use classical MD simulations to study the damage formation mechanisms in Si when depositing a given amount of energy in groups of neighboring atoms similar to those found in BCA calculations (Table I). In particular, we will focus on deposition conditions where the energy per atom is below E_d.

All our MD simulations are carried out in the NVE ensemble. Si-Si interactions are described using the Tersoff 3 potential.[22] Simulation cells are cubical and periodic boundary conditions are applied in all directions. Atoms located in a sphere in the center of the cell are given a certain kinetic energy with corresponding velocities in random directions. We will refer to these atoms as *initial moving atoms* [see Fig. 1(a)]. Their initial kinetic energies are chosen between 0 and 20 eV/atom, around and below the displacement threshold E_d routinely used in BCA simulators (15 eV). We have considered two different initial kinetic energy distributions. In the first one, each initial moving atom receives the same amount of kinetic energy, while in the second one the kinetic energy distribution is chosen according to the one found in the BCA groups. Total deposited energies range from 50 to 500 eV. We also analyze the case of 5 keV of total deposited energy to study the trend to the high energy regime. In those cases where the number of initial moving atoms is small, we run a total of 100 simulations for each set of initial conditions in order to improve statistics. All simulations are carried out at an initial temperature of 0 K to avoid damage migration and annihilation. The size of the simulation cell is chosen so that the final temperature increase in the MD cell is not enough to induce damage annealing ($\lesssim$70 K). Sizes range from 26 000 to 300 000 atoms depending on the total deposited energy.

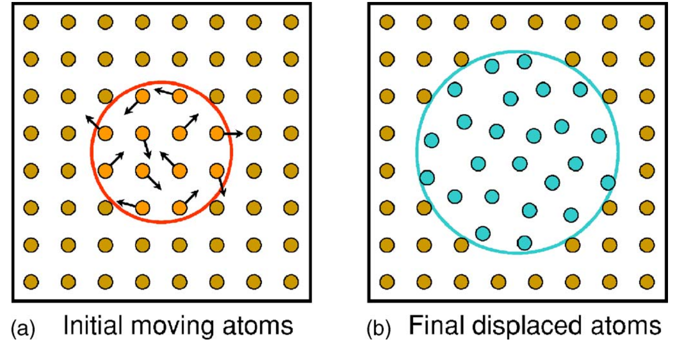

FIG. 1. (Color online) Schematic representation of the initial conditions (a) and final situation (b) in our MD simulations.

To identify damage zones in Si we have used a method based on the time average of atom coordinates,[23] which has been successfully employed to characterize self-interstitial configurations in Si.[24] Once the energy of the initial moving atoms has dissipated throughout the cell, the simulation continues over 1000 time steps during which atom positions are averaged in time. This procedure eliminates thermal vibrations and provides the local equilibrium positions for all atoms in the MD cell. Then, averaged atomic coordinates are compared with the original perfect lattice positions. When an atom is closer than 0.7 Å to a lattice site the atom is associated to that site, otherwise it is labeled as *displaced atom* and therefore it contributes to disorder [see Fig. 1(b)].

III. RESULTS AND DISCUSSION

We define the efficiency (eff) of damage generation as the final number of displaced atoms per initial moving atom. In the case of the KP model, $N_D=0.42F_D/E_d=0.42(N_I E_K)/E_d$, where N_I is the number of initial moving atoms and E_K is the mean initial kinetic energy per atom. The predicted efficiency is eff$=N_D/N_I=0.42E_K/E_d$, i.e., it does not depend on the total deposited energy. In the BCA model there is no damage production for energy densities below E_d (eff=0), and slightly over E_d just one atom is displaced because there is not enough energy to produce secondary recoils (eff=1). In Fig. 2 we represent our MD results on the efficiency of damage generation as a function of the initial kinetic energy per atom for different total deposited energies. Solid symbols correspond to simulations where all the initial moving atoms receive the same initial kinetic energy, and empty symbols to simulations with initial kinetic energy distributions consistent with the ones found in BCA groups. As can be seen, the initial energy distribution does not influence damage generation noticeably. This is because initial kinetic energy rapidly redistributes among the initial moving atoms long before damage generation takes place, as we will show later. Consequently, although the first type of MD simulations where all initial moving atoms start with the same kinetic energy may seem unrealistic, they can be used to obtain meaningful

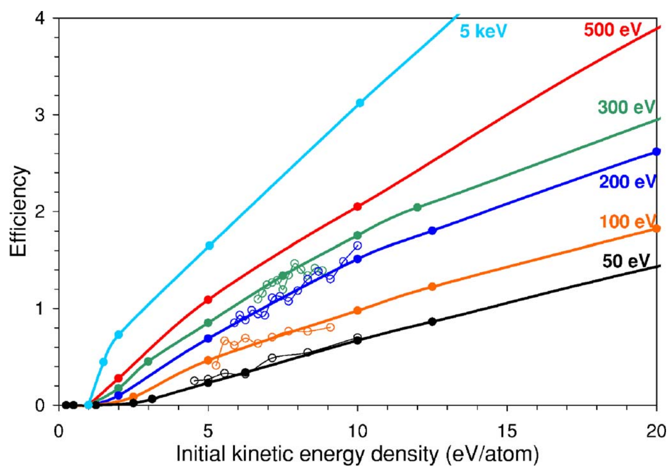

FIG. 2. (Color online) Efficiency of damage generation in MD as a function of the initial kinetic energy density for different total deposited energies. Solid and empty symbols represent results obtained with two different types of initial kinetic energy distributions (see text for details). Lines are to guide the eye.

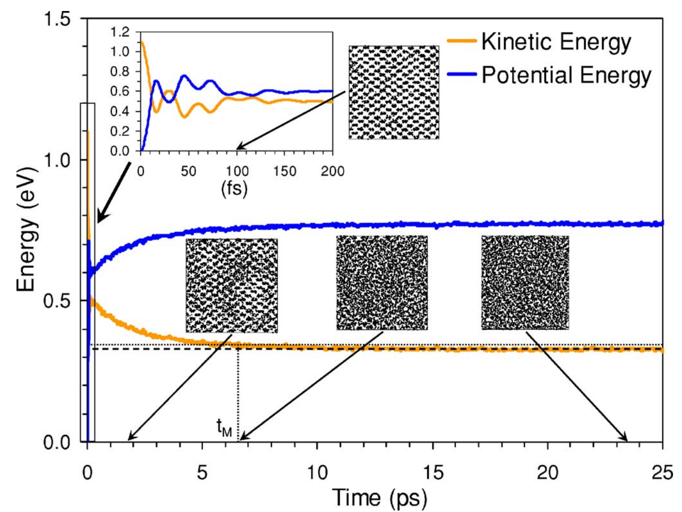

FIG. 3. (Color online) Average kinetic and potential energies per atom as a function of time for the simulation with an initial kinetic energy of 1.1 eV/atom. t_M is the time needed to melt. Cell snapshots correspond to the pointed times.

results. With respect to the efficiency of damage generation in MD, Fig. 2 shows that it increases with the initial kinetic energy density and also with the total deposited energy (unlike KP). Besides, efficiencies can be quite high for initial energy densities much below the displacement threshold E_d (unlike BCA). However, it is worth to note that in all cases no damage is generated at energy densities below $\sim$1 eV/atom even when the total deposited energy is as high as 5 keV.

To investigate the origin of this energy threshold at 1 eV/atom we have carried out MD simulations in which all atoms in the cell (and not only within a finite sphere) are given the same initial kinetic energy. The main difference with the MD simulations previously described is that now energy cannot dissipate to surrounding initially unexcited atoms. Consequently, all atoms in the MD cell maintain their total energy along the simulation, and only redistribution of this energy between kinetic and potential components is possible. We have simulated initial energy densities between 0.4 and 5 eV/atom. We observed that at initial kinetic energy densities below 0.6 eV/atom, deposited energy is equally redistributed between kinetic and potential components and no defects are generated. Between 0.6 and 1 eV/atom, the kinetic energy reach the value corresponding to the melting temperature, some defects are generated, but the cell is not fully disordered. In turn, for initial energy values of 1 eV/atom and above, the cell becomes completely disordered. Within the Tersoff 3 description of Si, $\sim$0.7 eV is the potential energy per atom in the liquid phase at the melting temperature referred to perfect crystal at 0 K, and $\sim$0.3 eV is the kinetic energy per atom corresponding to the melting temperature.[25] These energy values determine a threshold of $0.7+0.3=1$ eV/atom to fully disorder the MD cell. This is in fact a melting process: there must be in the cell the sufficient energy per atom to increase the temperature to the melting point (0.3 eV/atom) and to produce the phase change from crystal to liquid (0.7 eV/atom). It is worth to note however that this energy redistribution between kinetic and potential components does not occur instantaneously. As an example, in Fig. 3 we plot the evolution of the average kinetic and potential energies per atom referred to perfect crystal at 0 K in the simulation with an initial energy density of 1.1 eV/atom. The initial kinetic energy rapidly redistributes among the atoms, and after a few femtoseconds energy is equally divided between the kinetic and potential components. After this fast initial phase, some of the kinetic energy is converted to potential energy, indicating that a phase change starts to occur. Several picoseconds later, the cell reaches equilibrium and the average kinetic and potential energies per atom are 0.33 and 0.77 eV, respectively. The evolution of the simulation cell is shown in the snapshots of Fig. 3. During the initial phase atoms are vibrating although the cell remains ordered. At a time of 1.7 ps partial disorder can be observed and after 23.5 ps the melting process is fullfilled. To evaluate the time required to completely melt the cell, t_M, we have considered the instant when the average kinetic energy per atom differs 5% from its final equilibrium value. The corresponding snapshot shows that the cell is fully disordered at t_M. We have evaluated the pair distribution function to confirm that the cell effectively has the features of a liquid. We have found that t_M decreases rapidly when increasing the initial kinetic energy per atom, being 27 ps for an initial energy density of 1 eV/atom and only 35 fs for 4 eV/atom. It is worth to note that melting times t_M obtained in these MD simulations are the lowest ones for each deposited energy value, since there is no energy dissipation but only redistribution between the kinetic and potential components. These times are essential information as we will show later.

In a real cascade, groups of atoms that have received energies below E_d are surrounded by unexcited atoms, and energy out-diffusion occurs. The case of a limited number of excited atoms is illustrated with the simulation of 2500 initial moving atoms with an initial kinetic energy of 2 eV/atom, arranged in a sphere centered in a 300 000 atoms MD cell. In

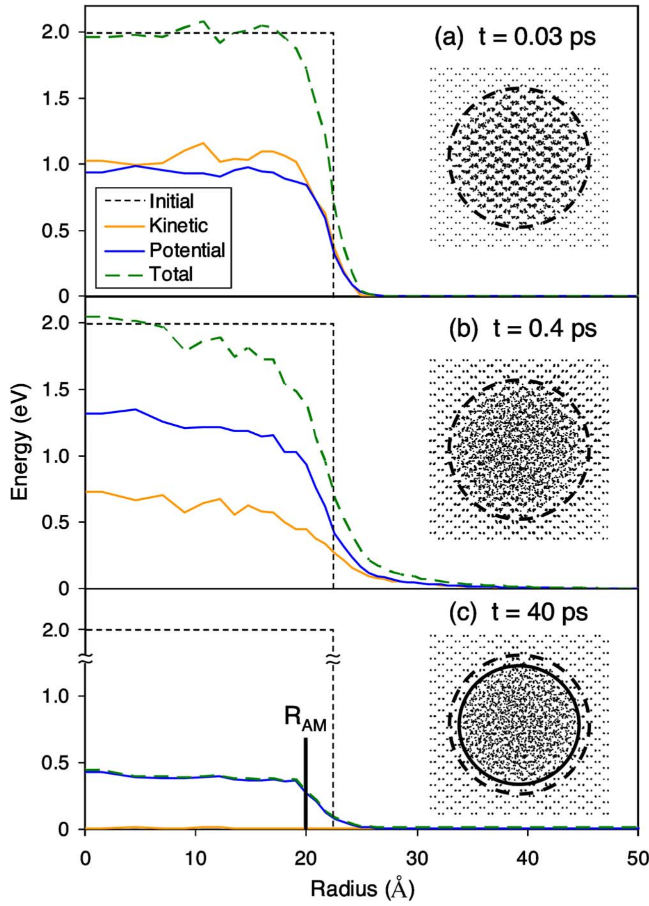

FIG. 4. (Color online) Kinetic, potential, and total energy radial profiles measured at different times for the simulation of 2500 atoms with an initial kinetic energy of 2 eV/atom. Corresponding cell snapshots are also shown. Black dashed lines indicate the initial energy profile and the radius of the sphere of initial moving atoms, and the black solid line in (c) the final amorphous radius, R_{AM}.

Fig. 4 we plot the mean kinetic, potential and total energy profiles as a function of the distance to the center of the simulation cell at different times. These profiles are consistent with a heat diffusion process[26] where thermal diffusivity decreases with temperature (as in real Si). At 30 fs, energy is equally distributed between kinetic and potential components and only a small part has diffused to atoms outside the initial sphere. The snapshot at this time shows that atoms are vibrating but the lattice keeps the crystal structure. After 400 fs, only atoms at the core of the sphere have a total energy of 2 eV as energy has diffused further to outer atomic shells. The energy distribution has changed: some of the kinetic energy has transformed into potential, which is consistent with a melting process. In fact, the corresponding snapshot shows a disordered region in the sphere core. At 40 ps, kinetic energy has fully dissipated throughout the cell and the potential profile shows the extent of the final amorphous region, R_{AM}. This finding is in agreement with direct cascade MD simulations, where amorphization caused by heavy ion implantation was attributed to the thermal spike[27] regime (melting and subsequent quenching) that follows the penetration of the ion within the target.[12] It is worth to note that although all the initial moving atoms have 2 eV of initial kinetic energy, twice the minimum energy value for melting, the final damage region is smaller than the initially perturbed volume. This observation suggests that 1 eV/atom is a necessary but not sufficient condition to assure the formation of amorphous pockets by a melting process. Consequently, solving the heat diffusion equation to determine atoms that have instantaneously reached an energy of 1 eV is not a valid criterion to evaluate the extent of amorphous regions.[20] This also explains why high temperature (>5000 K) shock waves generated by cluster implantation into Si do not produce melting during their propagation within the target.[14]

Simulation results presented so far suggest that the competition between melting and energy out-diffusion determines the formation of amorphous pockets. For a better understanding of this competition, we have analyzed MD simulations with the same total deposited energy, 5 keV, but with different initial kinetic energy values: 5, 2, and 1 eV/atom. In Fig. 5 we represent the time that the total energy of a shell of atoms is over a given value. Thick black solid line shows the melting times t_M, obtained from the simulations previously described, as a function of initial energy density. In the simulation of 1 eV/atom, all energy profiles fall on the left-hand side of t_M. In this case final damage

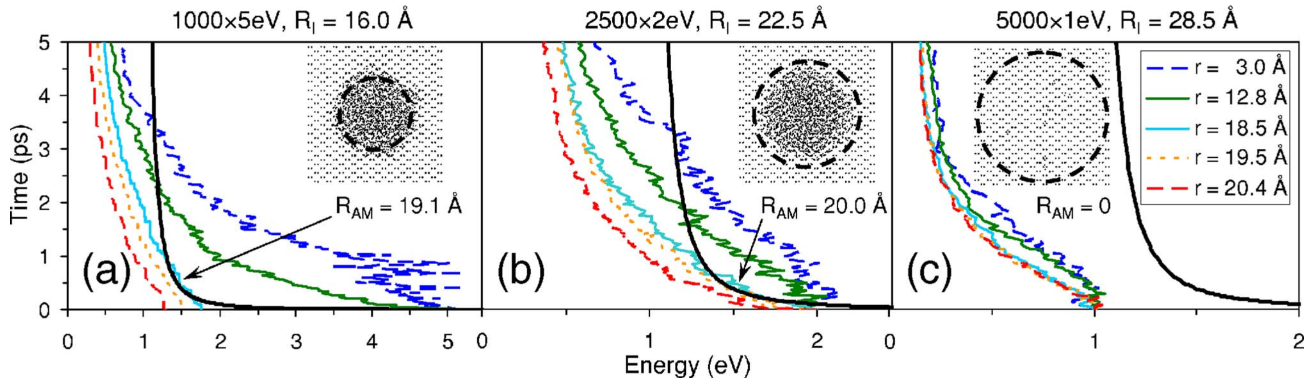

FIG. 5. (Color online) Time that the total energy of a shell of atoms at a certain distance from the center of the MD cell is over a given value. Initial conditions were (a) 1000 atoms with 5 eV/atom, (b) 2500 atoms with 2 eV/atom, and (c) 5000 atoms with 1 eV/atom. The radius of the sphere of initial moving atoms, R_I, and that of the final amorphous region, R_{AM}, are also indicated. Thick black solid line corresponds to the melting times t_M at each initial energy density. Snapshots show the final configurations.

consists of some isolated point defects as shown in the corresponding snapshot. On the contrary, for simulations of 5 and 2 eV/atom amorphization does take place, but the initial perturbation grows in the former and it shrinks in the latter. Only atomic shells whose total energy profile crosses to the right-hand side of the t_M line become disordered because atoms of these shells have enough energy for enough time to complete the melting process. Later on, remaining heat diffuses away leaving behind a supercooled liquid, which eventually becomes an amorphous pocket. These results have been obtained by the analysis of simulations with a high number of initial moving atoms in order to have good statistics. However, we have confirmed that they also hold for those with small number of initial moving atoms.

With these results about melting of the lattice and diffusion of local deposited energy we can understand better the efficiencies shown in Fig. 2. The efficiency of a simulation is zero when atoms have lost their energy too quickly to become disordered. For efficiencies below one, only atoms in the core of the excited region have enough energy during enough time to complete the melting process. In these cases, outer atoms have lost their energy so fast due to heat conduction that they cannot overcome the phase transition. In simulations with efficiencies over one, the energy of the excited region is so high that surrounding atoms receive enough energy for enough time to melt too. Our findings can explain the different damage morphology produced by different ions. For light ions, groups of atoms with energies below E_d formed during a cascade are small and their energy dissipates quickly. Then, damage production is not enhanced by this low-energy mechanism and it is mostly determined by ballistic processes. In the case of heavy ions, these groups are bigger and their energy remains concentrated longer. This favors melting, at least in the cascade core, and so they are more efficient in the formation of amorphous pockets.

IV. CONCLUSIONS

In conclusion, we have demonstrated that energy transfers below the displacement threshold can produce a significant amount of damage and should not be neglected in radiation damage calculations. The formation of amorphous pockets within this low-energy deposition regime is the result of a local melting, in agreement with the traditional concept of thermal spike. However, to complete this phase change, it is necessary to reach the appropriate kinetic-potential energy redistribution before deposited energy dissipates away. We have determined the minimum time needed for melting, and we have found that it is a fast decreasing function of the deposited energy density. Our findings explain the different damage morphology produced by different ions and can be used to develop an improved description of generated damage in BCA models.

ACKNOWLEDGMENTS

This work has been supported by the Spanish DGI under Project No. TEC2005-05101 and the JCyL Consejería de Educación y Cultura under Project No. VA070A05.

*Electronic address: ivasan@tel.uva.es

[1] P. Stolk, H. J. Gossmann, D. Eaglesham, D. Jacobson, C. Rafferty, G. Gilmer, M. Jaraíz, J. Poate, H. Luftman, and T. Haynes, J. Appl. Phys. **81**, 6031 (1997).
[2] S. Solmi, F. Baruffaldi, and R. Canteri, J. Appl. Phys. **69**, 2135 (1991).
[3] J. Ziegler, *The Stopping and Range of Ions in Solids* (Pergamon, New York, 1977), Vol. 1.
[4] M.-J. Caturla, T. Díaz de la Rubia, L. A. Marqués, and G. H. Gilmer, Phys. Rev. B **54**, 16683 (1996).
[5] P. Sigmund, Appl. Phys. Lett. **14**, 114 (1969).
[6] J. J. Loferski and P. Rappaport, Phys. Rev. **98**, 1861 (1955).
[7] M. Sayed, J. H. Jefferson, A. B. Walker, and A. G. Cullis, Nucl. Instrum. Methods Phys. Res. B **102**, 232 (1995).
[8] SRIM documentation, www.srim.org
[9] J. M. Hernández-Mangas, J. Arias, L. Bailón, M. Jaraíz, and J. Barbolla, J. Appl. Phys. **91**, 658 (2002).
[10] M. T. Robinson and I. M. Torrens, Phys. Rev. B **9**, 5008 (1974).
[11] S. E. Donnelly, R. C. Birtcher, V. M. Visnyakov, and G. Carter, Appl. Phys. Lett. **82**, 1860 (2003).
[12] T. Diaz de la Rubia and G. H. Gilmer, Phys. Rev. Lett. **74**, 2507 (1995).
[13] K. Nordlund, M. Ghaly, R. S. Averback, M. Caturla, T. Diaz de la Rubia, and J. Tarus, Phys. Rev. B **57**, 7556 (1998).
[14] S. Ihara, S. Itoh, and J. Kitakami, Phys. Rev. B **58**, 10736 (1998).
[15] K. M. Beardmore and N. Grønbech-Jensen, Phys. Rev. E **57**, 7278 (1998).
[16] J. Peltola, K. Nordlund, and J. Keinonen, Nucl. Instrum. Methods Phys. Res. B **195**, 269 (2002).
[17] International Technology Roadmap for Semiconductors, http://public.itrs.net
[18] J. F. Ziegler, J. P. Biersack, and U. Littmark, *The Stopping and Range of Ions in Solids* (Pergamon, New York, 1985).
[19] G. Hobbler and G. Otto, Nucl. Instrum. Methods Phys. Res. B **206**, 81 (2003).
[20] D. Kovač, G. Otto, and G. Hobler, Nucl. Instrum. Methods Phys. Res. B **228**, 226 (2005).
[21] I. Santos, L. A. Marqués, L. Pelaz, P. López, M. Aboy, and J. Barbolla, Mater. Sci. Eng., B **124-125**, 372 (2005).
[22] J. Tersoff, Phys. Rev. B **38**, 9902 (1988).
[23] L. A. Marqués, M. Caturla, T. D. de la Rubia, and G. Gilmer, J. Appl. Phys. **80**, 6160 (1996).
[24] L. A. Marqués, L. Pelaz, P. Castrillo, and J. Barbolla, Phys. Rev. B **71**, 085204 (2005).
[25] L. A. Marqués, L. Pelaz, M. Aboy, and J. Barbolla, Nucl. Instrum. Methods Phys. Res. B **216**, 57 (2004).
[26] N. A. Marks, Phys. Rev. B **56**, 2441 (1997).
[27] F. Seitz and J. S. Koehler, in *Solid State Physics: Advances in Research and Applications*, edited by F. Seitz and D. Turnbull (Academic, New York, 1956), Vol. 2, p. 305.